Efficiency of subset simulation in the design of lined rock caverns for storage of hydrogen gas

Davi R. Damasceno
PhD candidate, Div. of Soil and Rock Mechanics, KTH Royal Institute of Technology, Stockholm, Sweden

Johan Spross
Postdoctoral researcher, Div. of Soil and Rock Mechanics, KTH Royal Institute of Technology, Stockholm, Sweden

Fredrik Johansson
Associate professor, Div. of Soil and Rock Mechanics, KTH Royal Institute of Technology, Stockholm, Sweden

Jan Johansson
Licentiate of engineering, Naturgasteknik, Stockholm, Sweden

ABSTRACT: Efforts to substitute the use of fossil fuels in industry by hydrogen gas requires the storage of large volumes of gas with a reliable pressure vessel design. The Hydrogen Breakthrough Ironmaking Technology (HYBRIT) initiative aims to make the whole steel making process in Sweden fossil-free with the storage of industrial scale quantities of hydrogen in underground Lined Rock Cavers (LRCs). The LRC concept is a relatively new design methodology that can be further developed with respect to safety and economic efficiency and reliability-based design methods provide one option to comply with codes and regulations. High reliability is required for the storage of hydrogen gas and the computational time becomes unpractical for the evaluation of a complex system such as the LRC. In this paper, the efficiency of Subset Simulation (SuS) regarding accuracy, precision and required number of samples is studied for the calculation of probability of failure against fatigue of the steel lining. It can be observed that by increasing the number of samples per level and increasing the conditional probability of failure the precision increases as well as the total number of samples. The accuracy of the SuS is checked with respect to Monte Carlo simulation (MCS) showing good agreement and with greater precision for fewer number of samples. A case study is performed for the geologic conditions of Sweden showing that the considered failure mode is unlikely for high stresses and good rock mass quality.

1. INTRODUCTION

Major companies in Sweden (LKAB, SSAB and Vattenfall) are involved in the joint venture project titled Hydrogen Breakthrough Ironmaking Technology (HYBRIT) which aims to implement a fossil-free steel-making process in the Swedish industry. For this purpose, coal in the furnaces will be substituted by renewably produced and clean hydrogen gas. Large quantities of hydrogen must be readily available which can be solved by the use of industrial scale underground storages. Such underground storages enable the hydrogen production to be adjusted with respect to variations in electricity price, which makes the hydrogen gas more economically competitive. More information is available in the prestudy report written by Johansson et al. (2018).

Johansson (2003) proposed design principles for the construction of a Lined Rock Cavern (LRC), which were used for the demonstration project in Skallen, located on the west coast of Sweden (Johansson, 2003, Glamheden and Curtis, 2006, Tengborg et al., 2014). The main idea of this concept is that the lining keeps the storage gas-tight, while the surrounding rock mass provides confining pressure to prevent excessive deformation of the lining during gas filling of the storage. The LRC is composed by a rock cavern covered by a special purpose shotcrete with a built-in drainage system, followed by a reinforced concrete lining, sliding layer and steel lining, as shown in Figure 1.

The current design methodology for LRCs is based on simplifications regarding the consideration of anisotropic stresses, influence of three-dimensional geometry and straining at any point around the storage, which requires the use of correction factors that are project dependent. Less simplified problems, for which analytical solutions are not available, require the use of three-dimensional Finite Element Modeling (FEM); however, FE-based methods used for the LRC design in Skallen are also oversimplified. Updates on the current knowledge and development of the LRC's safety and economic design are expected to benefit the HYBRIT initiative.

The natural variability of the rock mass properties introduces uncertainty to the LRC design and no specific guidelines are available for addressing this heterogeneity. For example, codes and regulations, such as the Eurocode, suggest acceptable failure probability for structures ranging from 10^{-5} to 10^{-7} depending on the magnitude of failure consequences; therefore, a reliability-based approach is used in this paper to address the LRC design uncertainties to satisfy these probability of failure magnitudes.

However, such low probabilities of failure require significant amount of sampling to evaluate the desired failure probability and this

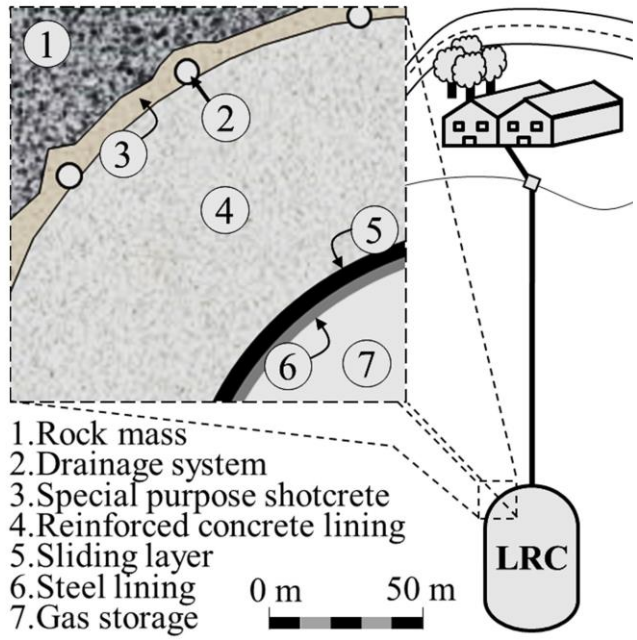

Figure 1: Components of the LRC concept.

process becomes prohibitive if the response of the system is difficult to evaluate, e.g. using FEM. Thus, the efficiency of the reliability-based method needs to be increased with respect to required number of samples to achieve acceptable accuracy and precision as each sample will correspond to one FEM simulation.

In this paper, the efficiency regarding accuracy, precision and number of samples of Subset Simulation (SuS) is studied and compared with Monte Carlo simulation (MCS).

2. RELIABILITY ANALYSIS FOR LRC

The reliability of a structure is often expressed by the probability of failure. The true probability of failure, p_{f}, is defined as the probability of the response of the system to be negative, $M(\boldsymbol{X}) < 0$, that corresponds to the integral of the probability density function, $f_{\boldsymbol{X}}(\boldsymbol{x})$, in that region:

$$p_{\mathrm{f}} = P(M(\boldsymbol{X}) < 0) = \int_{M(\boldsymbol{X})<0} f_{\boldsymbol{X}}(\boldsymbol{x}) dx \qquad (1)$$

Detailed explanations for different reliability analysis methods is presented in e.g. Baecher and Christian (2003) and Melchers and Beck (2018).

In this section the MCS and SuS concepts are explained as well as the definition of the limit-state function.

2.1. Monte Carlo simulation

The MCS is a simple and robust sampling method that is used to numerically approximate integrals and expected values. The evaluation of the probability of failure, $\hat{p}_{\mathrm{f}}$, considers sampling in the whole system domain and counting the number of failed responses, n_{f}, represented by

$$\hat{p}_{\mathrm{f}} = \frac{n_{\mathrm{f}}}{n} \tag{2}$$

where n is the total number of samples. The convergence for the approximated probability of failure using MCS is calculated by its coefficient of variation, COV, as a function of p_{f} and n:

$$COV(\hat{p}_{\mathrm{f}}) = \sqrt{\frac{1 - p_{\mathrm{f}}}{n\, p_{\mathrm{f}}}} \tag{3}$$

It can be noted that the number of samples required for acceptable convergence is inversely proportional to the actual probability of failure and the use of MCS may be unpractical if this probability of failure is very low. Variance reduction techniques are available to minimize the number of times that the response of the system needs to be evaluated for acceptable convergence of result.

2.2. Subset Simulation

Au and Wang (2014) explain the details of SuS. SuS efficiently approximates small probabilities of failure by expressing a rare event as a product of m more frequent intermediate events, F_i:

$$p_{\mathrm{f}} = P\left(\bigcap_{i=1}^{m} F_i\right) = \prod_{i=1}^{m} P(F_i | F_{i-1}) \tag{4}$$

This method is robust and does not require any prior information about the system behavior; e.g. importance sampling methods require prior knowledge about the shape of the probability density function of the system response. A predefined number of samples is generated per level, n_{L}, in the unconditional level through standard MCS and the first intermediate threshold (L_1, as in Figure 2) is set at the percentile of the responses corresponding to the defined conditional probability of failure, p_{c}. More samples are then adaptively generated through Markov chains conditioned to the failed responses and a new intermediate threshold, L_i, is set. This process is repeated until the intermediate threshold becomes negative and the approximation for the probability of failure is calculated by:

$$\hat{p}_{\mathrm{f}} = p_{\mathrm{c}}^{m-1}\left(\frac{n_{\mathrm{f}m}}{n_{\mathrm{L}}}\right) \tag{5}$$

where $n_{\mathrm{f}m}$ is the number of failed responses at the last level m in which the SuS converged.

2.3. Limit-state function

In the present paper, steel lining fatigue failure caused by the pressure cycles in the LRC is evaluated at the middle horizontal cross-section of the cylindrical cavern (plane-strain simplification). It is assumed that the cracks in the concrete lining are well distributed and that there is no concentration of deformation at individual joints located in the rock mass. The limit-state function, $M_{\mathrm{f}} = 0$, is set as the fatigue resistance of the steel, R_{f}, subtracted the fatigue load applied by the cyclic pressurization of the storage, S_{f}, expressed in strain ranges by:

$$M_{\mathrm{f}} = R_{\mathrm{f}} - S_{\mathrm{f}} = \Delta\varepsilon_{\mathrm{R}} - \Delta\varepsilon_{\mathrm{S}} \tag{6}$$

The strain range resistance, $\Delta\varepsilon_{\mathrm{R}}$, is defined by Morrow's relation:

$$\frac{\Delta\varepsilon_{\mathrm{R}}}{2} = \frac{\sigma_{\mathrm{f}}'}{E_s}(2N_{\mathrm{f}})^b + \varepsilon_{\mathrm{f}}'(2N_{\mathrm{f}})^c \tag{7}$$

where σ_{f}' is the fatigue strength coefficient, E_{s} is the Young's modulus of the steel, N_{f} is the total number of cycles expected for the LRC life-span, b is the fatigue strength exponent, $\varepsilon_{\mathrm{f}}'$ is the fatigue ductility coefficient and c is the fatigue ductility exponent.

The strain range load, $\Delta\varepsilon_{\mathrm{S}}$, is calculated by the difference between the tangential strains, ε_{t}, at the maximum and minimum operational internal pressures, p_{i}, of the LRC, which for this calculation was set to 20 MPa and 3 MPa, respectively:

$$\Delta\varepsilon_{\mathrm{S}} = \varepsilon_{\mathrm{t}}^{\{20\mathrm{MPa}\}} - \varepsilon_{\mathrm{t}}^{\{3\mathrm{MPa}\}} \tag{8}$$

The thickness of the concrete lining is fixed for any LRC size, so for a large scale LRC, the concrete lining contribution to the global straining is relatively small. In addition, it is assumed that the steel lining does not resist any deformation, thereby following the same behavior as the rock mass shown by Johansson et al. (1995). These equations were derived from the standard convergence–confinement method found in textbooks such as Palmström and Stille (2015), but considering internal pressure inside the cavern. The tangential strain behavior may be compressive elastic, ε_{E}, tensile elastic, ε_{T}, or compressive plastic, ε_{P}, and must be evaluated for each combination of random variables depending on the following inequalities:

$$\varepsilon_{\mathrm{t}} = \begin{cases} \varepsilon_{\mathrm{E}} & \text{if} \quad p_{\mathrm{i}} \leq p_{\mathrm{e}} \\ \varepsilon_{\mathrm{T}} & \text{if} \quad p_{\mathrm{e}} < p_{\mathrm{i}} \leq \sigma_{\mathrm{c}} \\ \varepsilon_{\mathrm{P}} & \text{if} \quad p_{\mathrm{i}} > \sigma_{\mathrm{c}} \end{cases} \tag{9}$$

where p_{e} is defined as $2p_{\mathrm{o}} + \sigma_{\mathrm{o}}$, in which p_{o} is the initial isotropic stress and σ_{o} is the tensile strength of the rock mass, and σ_{c} is the compressive strength of the rock mass.

If $p_{\mathrm{i}} \leq p_{\mathrm{e}}$, the tangential strain is compressive elastic and calculated by:

$$\varepsilon_{\mathrm{E}} = \frac{1+v_{\mathrm{r}}}{E_{\mathrm{r}}} p_{\mathrm{i}} \tag{10}$$

where v_{r} is the Poisson ratio and E_{r} is the Young's modulus of the rock mass. In the case of $p_{\mathrm{e}} < p_{\mathrm{i}} \leq \sigma_{\mathrm{c}}$, the cracks in the rock begin to open and tensile straining takes place:

$$\begin{aligned} \varepsilon_{\mathrm{T}} = -\frac{1+v_{\mathrm{r}}}{E_{\mathrm{r}} r_{\mathrm{i}}} \big(p_{\mathrm{o}}(2r_{\mathrm{T}}(1-v_{\mathrm{r}}) \\ - (1-2v_{\mathrm{r}})r_{\mathrm{i}}) - p_{\mathrm{e}} r_{\mathrm{T}} \\ + p_{\mathrm{i}}(1-v_{\mathrm{r}}) r_{\mathrm{i}} \ln(r_{\mathrm{i}}/r_{\mathrm{T}}) \\ - p_{\mathrm{o}} r_{\mathrm{i}}\big) \end{aligned} \tag{11}$$

where

$$r_{\mathrm{T}} = r_{\mathrm{i}} p_{\mathrm{i}} / p_{\mathrm{e}} \tag{12}$$

in which r_{i} is the internal radius of the storage.

If $p_{\mathrm{i}} > \sigma_{\mathrm{c}}$, shear failure occurs in the rock mass causing plastic behavior:

$$\varepsilon_{\mathrm{P}} = \left(\left(u_{\mathrm{t}} - B r_{\mathrm{P}}\right) r_{\mathrm{P}}^{1/f}\right) r_{\mathrm{i}}^{\frac{-1-f}{f}} + B \tag{13}$$

where

$$\begin{aligned} u_{\mathrm{t}} = -\frac{1+v_{\mathrm{r}}}{E_{\mathrm{r}}} \big(p_{\mathrm{o}}(2r_{\mathrm{D}}(1-v_{\mathrm{r}}) \\ - (1-2v_{\mathrm{r}})r_{\mathrm{P}}) - p_{\mathrm{e}} r_{\mathrm{D}} \\ + p_{\mathrm{g}}(1-v_{\mathrm{r}})\, r_{\mathrm{P}} \ln(r_{\mathrm{P}}/r_{\mathrm{D}}) \\ - p_{\mathrm{o}} r_{\mathrm{i}}^2 / r_{\mathrm{P}}\big) \end{aligned} \tag{14}$$

$$B = \frac{-f\varepsilon_{\mathrm{r,el}} - \varepsilon_{\mathrm{t,el}}}{1+f} \tag{15}$$

$$r_{\mathrm{P}} = r_{\mathrm{i}} \left(\frac{a_{\mathrm{r}}(k_{\mathrm{r}}-1)}{p_{\mathrm{i}}}\right)^{-\frac{k_{\mathrm{r}}}{k_{\mathrm{r}}-1}} \tag{16}$$

$$f = \frac{\tan(45 + \varphi_{\mathrm{r}}/2)}{\tan(45 + \varphi_{\mathrm{r}}/2 - \psi)} \tag{17}$$

in which

$$r_{\mathrm{D}} = r_{\mathrm{P}} p_{\mathrm{g}} / p_{\mathrm{e}} \tag{18}$$

$$p_{\mathrm{g}} = a_{\mathrm{r}}(k_{\mathrm{r}} - 1) \tag{19}$$

$$a_{\mathrm{r}} = c_{\mathrm{r}} / \tan(\varphi_{\mathrm{r}}) \tag{20}$$

$$k_{\mathrm{r}} = \tan^2(45 + \varphi_{\mathrm{r}}/2) \tag{21}$$

$$\begin{aligned} \varepsilon_{\mathrm{r,el}} = \frac{1+v_{\mathrm{r}}}{E_{\mathrm{r}}} \big(-p_{\mathrm{o}}(1-2v_{\mathrm{r}}) \\ + p_{\mathrm{g}}(1-v_{\mathrm{r}}) \\ + p_{\mathrm{o}}(r_{\mathrm{i}}/r_{\mathrm{P}})^2\big) \end{aligned} \tag{22}$$

$$\begin{aligned} \varepsilon_{\mathrm{t,el}} = \frac{1+v_{\mathrm{r}}}{E_{\mathrm{r}}} \big(-p_{\mathrm{o}}(1-2v_{\mathrm{r}}) - v_{\mathrm{r}} p_{\mathrm{g}} \\ - p_{\mathrm{o}}(r_{\mathrm{i}}/r_{\mathrm{P}})^2\big) \end{aligned} \tag{23}$$

where c_{r} is the residual cohesion, φ_{r} is the residual friction angle and ψ is the dilatancy angle. The field data from the LRC demonstration project in Skallen (Mansson et al., 2006) shows that the strain range after a few cycles tends to decrease in magnitude due to compaction of the rock mass; therefore, the strain calculations for the first cycle performed in this paper can be considered conservative.

3. EFFICIENCY OF SUBSET SIMULATION

The variables for steel lining and rock mass are defined as well as the considered cases for combinations of SuS parameters. The probability of failure for the steel lining of the LRC is evaluated for SuS and the efficiency with respect to accuracy, precision and number of samples is compared for SuS and MCS. In order to enable comparison of the simulation methods around the target probability of failure (10^{-5}), rather unfavorable rock mass conditions were selected. For reference, the probability of failure is evaluated also for typical Swedish conditions in section 3.3.

3.1. Limit-state variable definition and SuS cases

The means, μ, and coefficient of variations, COV, of the fatigue properties of the steel lining and rock mass parameters are defined in Table 1. The fatigue properties follow the definitions in de Jesus et al. (2012) for conventional steel grade S355 and it is assumed that they are either constant or varying with 5% COV. The mean values of isotropic stress and rock mass properties are based on Johansson et al. (1995), the variations for stress are taken from Stephansson (1993) and the variations of rock mass properties are taken from Glamheden et al. (2007). The radius of the LRC is the same as the one for the demonstration project in Skallen (Johansson, 2003) and the number of cycles for the storage life-span corresponds to HYBRIT's preliminary assumptions of about one cycle per week (Johansson et al., 2018) assuming a period of 16.35 years. Parameters with variation

Table 1: Fatigue properties of steel and rock mass parameters including mean, coefficient of variation and distribution type.

Variable	μ	COV	Distribution
r_{i}[m]	18	0.05	Normal
N_{f}	850	-	-
E_{s}[GPa]	210	0.05	Normal
σ_{f}'[MPa]	952	0.05	Normal
b	-0.089	-	-
$\varepsilon_{\mathrm{f}}'$	0.74	0.05	Normal
c	-0.66	-	-
p_{o}[MPa]	2	0.28	Lognormal
E_{r}[GPa]	40	0.12	Normal
υ_{r}	0.2	0.12	Normal
σ_{c}[MPa]	10	0.46	Lognormal
σ_{o}[MPa]	0.1	0.68	Lognormal
c_{r}[MPa]	2.5	0.25	Lognormal
φ_{r}[°]	35	0.10	Normal
ψ[°]	10	0.65	Lognormal

lower than 15% are assumed to be normally distributed while other variables have a lognormal distribution.

The efficiency of SuS is evaluated with respect to the number of samples per level, n_{L}, and conditional probability of failure, p_{c}. The combination of these variables is presented by 9 cases in Table 2. The simulations are evaluated for 100 repetitions in order to obtain some statistical significance. The mean of the approximated probabilities of failure, $\bar{p}_{\mathrm{f}}$, and its coefficient of variation, as well as the average total number of samples, $\bar{n}$, are calculated.

Table 2: SuS case definition for different n_{L} and p_{c}.

Case	n_{L}	p_{c}
1	500	0.10
2	500	0.25
3	500	0.50
4	1 000	0.10
5	1 000	0.25
6	1 000	0.50
7	5 000	0.10
8	5 000	0.25
9	5 000	0.50

3.2. Results from SuS cases

Since the estimations for probability of failure are being averaged based on 100 repetitions of the simulations, increasing accuracy for each individual simulation with increasing precision is expected. The true value of the probability of failure, $\bar{p}_{\mathrm{ft}}$, is approximated by the MCS for 10^8 samples and corresponds to $1.40\text{x}10^{-5}$ with $COV \approx 2.5\%$. The efficiency for SuS is evaluated with respect to the error, ξ, as:

$$\xi = \frac{|\bar{p}_{\mathrm{ft}} - \bar{p}_{\mathrm{f}}|}{\bar{p}_{\mathrm{ft}}} \tag{24}$$

The error is calculated with respect to averaging of probabilities of failure of 100 trials which corresponds to more accurate results than the accuracy from single approximations. Table 3 lists the results for each considered case for ξ, COV, and $\bar{n}$.

The acceptable precision is assumed to correspond to the average variation of the highest uncertainties that relate to the rock mass parameters ($COV = 33\%$); therefore, case 8 is a good SuS setup for this example. Figure 2 illustrates the progressive sampling and amount of levels that were generated before reaching the limit-state, for case 8. All simulations have a relatively low error for 100 repetitions; however, the precision varies significantly, having the largest coefficient of variation of 189% for case 1 (small n_{L} and low p_{c}) and smallest coefficient of variation of 16% for case 9 (large n_{L} and high p_{c}). The required amount of samples is inversely proportional to the variation of the approximations, giving the fewest number of samples for case 1 and the largest for case 9.

Table 3: ξ, COV and $\bar{n}$ for each simulation case.

Case	ξ[%]	COV[%]	$\bar{n}$
1	4	189	2 805
2	12	96	4 430
3	7	40	8 410
4	4	167	5 600
5	5	55	8 730
6	2	35	16 720
7	2	48	26 550
8	1	29	43 550
9	3	16	83 400

Figure 2 can be compared to Figure 3, which illustrates the sampling scheme for MCS with limit-state line and PDF contour. It can be seen that for MCS, a very large number of simulations was necessary for merely a few samples to appear in the failure region.

Considering case 8 for SuS, the efficiency with respect to accuracy, precision and required number of samples is compared with MCS for the coefficient of variation and total number of samples. The expected number of samples to achieve similar COV in MCS as SuS is approximated from equation 3 as $\bar{n}$ = 825 594. Table 4 shows the compilation of results for the comparison between SuS and MCS. These results show that in order to achieve similar COV, MCS must use about 20 times the number of samples in SuS while the use of same $\bar{n}$ as SuS results in a variation about 4.5 times greater, causing poorer accuracy for MCS.

3.3. Simulation results using typical Swedish Conditions

For the purpose of HYBRIT, the geologic conditions of Sweden, which correspond to very good rock mass quality, should be taken into account. Table 5 shows the isotropic stress at 100 meters depth from overcoring measurements in the Baltic shield (Stephansson, 1993) and parameters for granitic rock mass achieved from the software RocData (Rocscience) for Geological Strength Index (GSI) between 60 and 80. These rock conditions are significantly better than the ones considered in section 3.

The approximated probability of failure using SuS with the same setup as case 8 for these geologic conditions shows extremely low

Table 4: Comparison of case 8 of SuS and MCS with respect to similar COV and $\bar{n}$.

Method	ξ[%]	COV[%]	$\bar{n}$
$\mathrm{SuS}_{\mathrm{case8}}$	1	29	43 550
$\mathrm{MCS}_{\mathrm{SuS}COV}$	2	31	825 594
$\mathrm{MCS}_{\mathrm{SuS}n}$	12	138	43 550

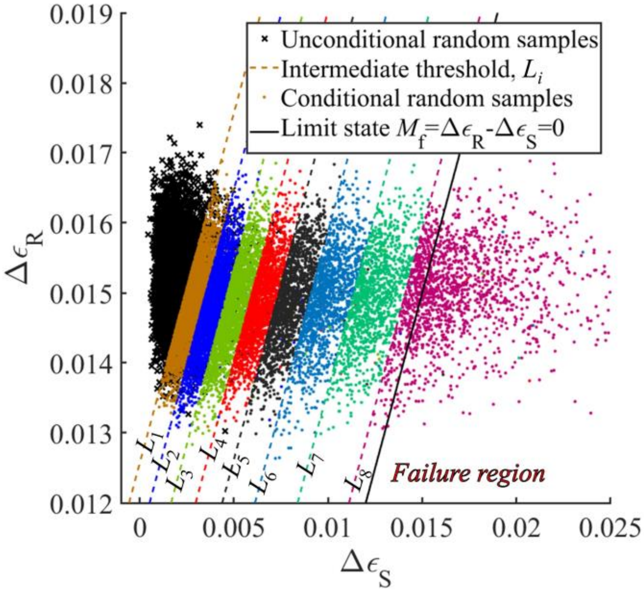

Figure 2: SuS for a total of 4.5x10⁴ samples with n_L=5 000 and p_c=0.25 (case 8). The samples from the unconditional level are generated from MCS as black "x" markers. Random samples are generated as dots with the same color as their corresponding intermediate thresholds, L_i, and are forced toward the true failed region. Samples at higher levels are overlaying the ones from lower levels.

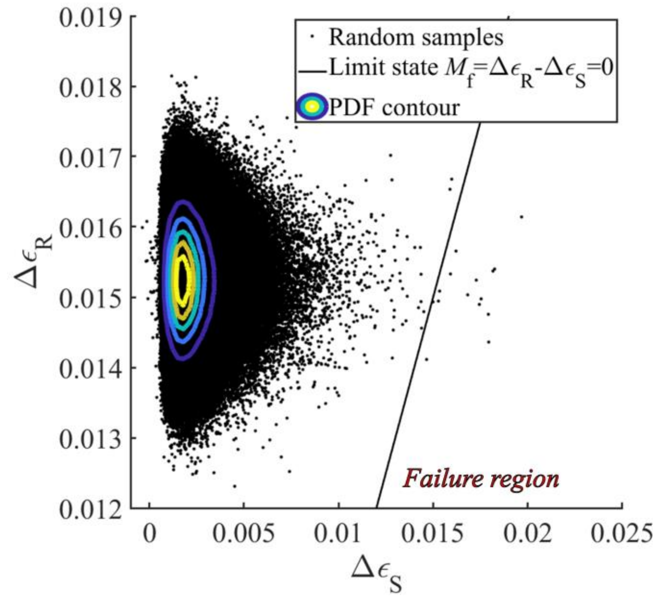

Figure 3: MCS for 10^6 samples. The region of highest concentration of samples is shown by the PDF contour. The limit-state line delimitates the region of failed samples.

probability of failure ($\bar{p}_f$ = 2.44x10^{-16}) and large variation in this estimation (COV= 518%). This $\bar{p}_f$ is far below the magnitudes specified in codes and regulations (10^{-5} to 10^{-7}) and the large variation shows difficulty for convergence due to extremely low true probability of failure. Fatigue failure of the steel lining for the geologic conditions of Sweden would be unlikely for the considered model, which does not take into account the local straining caused by opening of cracks in the concrete (description in Johansson et al. (1995)).

Table 5: Mean values for parameters representing stress magnitudes in the Baltic shield and granitic rock mass.

Variable	μ
p_o[MPa]	7.62
E_r[GPa]	77.86
σ_c[MPa]	47.01
σ_o[MPa]	0.81

4. CONCLUSIONS

The efficiency of SuS regarding accuracy, precision and required number of samples was reviewed for the probability of failure against steel lining fatigue of LRCs. The averaging of 100 outcomes results in fairly accurate approximations for the true MCS probability of failure with average error of about 4.5%. Increasing the number of samples per level and conditional failure probability results in more precise approximations with larger amount of required number of samples. The MCS comparison with SuS results in the requirement of 20 times more samples to achieve similar precision and 4.5 more variation when using the same number of samples as SuS. However, the required number of samples for SuS still seem quite large for the use with FEM; therefore, other approaches such as the Response Surface Method will also be reviewed in future studies.

For the geologic conditions of Sweden, the probability of failure against fatigue of the LRC approximated by SuS is negligible compared to regulation requirements, despite local strains were not considered, e.g. opening of joints in the rock mass and cracks in the concrete because of the gas pressure. These local effects must be accounted for as they will increase the risk for low cycle fatigue. Regarding the steel lining, laboratory tests should be performed using welded samples as required by the LRC design. Embrittlement of the steel because of hydrogen may also be a concern that needs further research. Once an efficient reliability model is set for the present study, further development of the LRC design methodology regarding material optimization and allowable number of pressurization cycles can be proposed.

ACKNOWLEDGMENT
This work has been conducted as part of the HYBRIT research project RP-1. The authors gratefully acknowledge the financial support from the Swedish Energy Agency.

5. REFERENCES

Au, S., and Wang, Y. (2014). *Engineering risk assessment with subset simulation.* Wiley, Singapore.

Baecher, G. B., and Christian, J. T. (2003). *Reliability and statistics in geotechnical engineering*. Wiley, Chichester.

de Jesus, A. M. P., Matos, R., Fontoura, B. F.C., Rebelo, C., da Silva, L. S., and Veljkovic, M. (2012). “A comparison of the fatigue behavior between S355 and S690 steel grades.” *Journal of Constructional Steel Research*, 79, 140-150.

Glamheden, R., and Curtis, P. (2006). “Excavation of a cavern for high-pressure storage of natural gas.” *Tunnelling and Underground Space Technology*, 21, 56-67.

Glamheden, R., Fredriksson, A., Röshoff, K., Karlsson, J., Hakami, H., and Christiansson, R. (2007). *Rock Mechanics Forsmark Site descriptive modelling Forsmark stage 22*. R-07-31, SKB, Stockholm.

Johansson, F., Spross, J., Damasceno, D., Johansson, J., and Stille, H. (2018). *Investigation of research needs regarding the storage of hydrogen gas in lined rock caverns: Prestudy for Work Package 2.3 in HYBRIT Research Program 1.* TRITA-ABE-RPT-182, KTH Royal Institute of Technology, Stockholm.

Johansson, J. (2003). *High pressure storage of gas in lined rock caverns, cavern wall design principles*. TRITA-JOB LIC 2004, KTH Royal Institute of Technology, Stockholm.

Johansson, J., Stille, H., and Sturk, R. (1995). *Pilotanläggning för inklädda gaslager i Grängesberg – Fördjupad analys av försöksresultaten*. TRITA-AMI REPORT 3004, KTH Royal Institute of Technology, Stockholm.

Mansson, L., Marion, P., and Johansson, J. (2006). “Demonstration of the LRC gas storage concept in Sweden.” *Proceedings of the World Gas Conference, Amsterdam, 5-9 June 2006*. Barcelona: International Gas Union, 1-17.

Melchers, R. E., and Beck, A. T. (2018). *Structural reliability analysis and prediction.* Wiley, Hoboken.

Palmström, A., and Stille, H. (2015). *Rock Engineering.* Institute of Civil Engineers, London.

Stephansson, O. (1993). “Rock Stress in the Fennoscandian Shield.” *Comprehensive Rock Engineering*, 3, 446-459.

Tengborg, P., Johansson, J., and Durup, J. G. (2014). “Storage of highly compressed gases in underground Lined Rock Caverns – More than 10 years of experience.” *Proceedings of the World Tunnel Congress, Foz do Iguaçu, 9-15 May 2014.*